Entropy
ISSN 1099-4300
www.mdpi.org/entropy/

Full Paper

Second Law Analysis of Laminar Flow In A Channel Filled With Saturated Porous Media

O.D. Makinde and E. Osalusi

Applied Mathematics Department, University of Limpopo,
Private Bag X1106, Sovenga 0727, South Africa

Received: 10 March 2005 / Accepted: 16 May 2005 / Published: 19 May 2005

Abstract: The entropy generation rate in a laminar flow through a channel filled with saturated porous media is investigated. The upper surface of the channel is adiabatic and the lower wall is assumed to have a constant heat flux. The Brinkman model is employed. Velocity and temperature profiles are obtained for large Darcy number (D_a) and used to obtain the entropy generation number and the irreversibility ratio. Generally, our result shows that heat transfer irreversibility dominates over fluid friction irreversibility (i.e. $0 \leq \phi < 1$), and viscous dissipation has no effect on the entropy generation rate at the centerline of the channel.

Keywords: Laminar flow, Porous medium, Entropy generation, Irriversibility ratio

---

Nomenclature

a	channel width
B_r	Brinkman number
c_p	specific heat at constant pressure
D_a	Darcy number
G	applied pressure gradient
k	fluid thermal conductivity
K	Permeability
M	μ_e/μ
P_e	Peclet number
q	fluid flux rate
s	$(MDa)^{-1/2}$)
T_0	wall temperature
T	absolute temperature
U	dimensionless fluid velocity
u	dimensionless fluid velocity as $s \to 0$
$\bar{u}$	fluid velocity
x	dimensionless axial coordinate
y	dimensionless transverse coordinate
$\bar{x}$	axial coordinate
$\bar{y}$	transverse coordinate
Greek symbols	
μ	fluid viscosity
μ_e	effective viscosity in the Brinkman term
θ	dimensionless temperature
Ω	dimensionless temperature difference qa/kT_0
ρ	fluid density

Introduction

Studies related to laminar flow in a channel filled with saturated porous media have increased significantly during recent years. This type of geometry and flow configuration are commonly observed in field of electronics cooling system, solid matrix heat exchanger, geothermal system, nuclear waste disposal, microelectronic heat transfer equipment, coal and grain storage, petroleum industries, and catalytic converters. Meanwhile, the improvement in thermal systems as well as energy utilization during the convection in any fluid is one of the fundamental problems of the engineering processes, since improved thermal systems will provide better material processing, energy conservation and environmental effects, (Makinde, [12]).

Another potential application of convection processes in porous media is found in thermoacoustic prime movers and heat pumps (Rott [15], Swift [20]), where the fluid-gap within stacks of a thermoacoustic engine/refrigerator are treated as porous media. Thermoacoustic engines are devices which make use of the thermoacoustic phenomena and function as heat pumps or prime movers. They can provide cooling or heating using enviromentally benign gases (such as oxygen or nitrogen) as the working fluid. Despite recent developments in thermoacoustic engines (see Swift [20]), there are many areas requiring further investigation in order to better predict their performance and guide future designs for thermoacoustic engines. Any thermoacoustic device (system) can be divided into four basic components (resonant tube, speaker, heat exchangers, and regenerator or stacks);among them the stack serves as the heart of the thermoacoustic device. In engine and heat pump, stacks are finely subdivided into many parallel channels or pores. Starting from the single plate, stacks are available in different sizes and shapes. Multi-plate arrays, honeycombs, spiral roles, and pin arrays' are some example of stacks commonly used in thermoacoustics engines and refrigerators. (see Swift [20]). To improve the thermal contact and heat transfer area, a porous medium (a fine wire mesh made of a material with moderate to good thermal conductivity) of moderate permeability may be embedded inside the fluid gap between two consecutive stacks. Most of the existing theories (of thermoacoustics engines/prime movers) consider a non-porous medium and very few of them use a single pore (of circular or square cross-section) to model thermoacoustic systems. In thermoacoustic devices, stacks are repeated along the transverse direction of fluid motion. The fluid gap between two consecutive stacks is usually kept constant. Two consecutive stacks plates and the fluid gap may be approximated as a unit-channel and inside the resonant chamber the stack (or regenerator) consists of many unit-channels. The fluid dynamics of all unit-channel must be similar (neglecting resonant chamber wall effects). Therefore, this present research can be applicable to one unit-channel.

One of the methods used for predicting the performance of the engineering processes is the second law analysis. The second law of thermodynamics is applied to investigate the irreversibilities in terms of the entropy generation rate. Since the entropy generation is the measure of the destruction of the available work of the system, the determination of the active sites motivating the entropy generation is also important in upgrading the system performances. This method was introduced by Bejan[2,3,4] and followed by many other investigators e.g. Arpaci[1], Sahin[14],Sahin[16],Narusawa[13], Erbay et al.[6],Mahmud and Fraser[9], Sahin[16], Salah et al.[18]. In this present paper, special attention has been given to the effect of porous medium permeability on the entropy generation and irreversibility ratio.

Mathematical Formulation

For the steady-state hydrodynamically developed situation we have unidirectional flow in the $\bar{x}$-direction between impermeable boundaries at $\bar{y} = 0$ and $\bar{y} = a$, as illustrated in Fig.1. The channel is composed of a fixed lower heated wall with constant heat flux while the upper wall is fixed and adiabatic. Other physical properties of the fluid like viscosity and density are taken as constant.

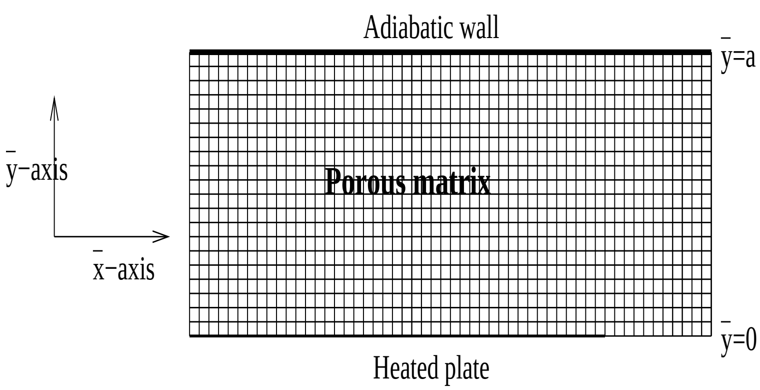

Figure 1: Geometry of the problem

The Brinkman momentum equation is

$$\mu_e \frac{d^2\bar{u}}{dy^2} - \frac{\mu}{K}\bar{u} + G = 0, \quad \bar{u}(0) = 0, \quad \bar{u}(a) = 0, \tag{1}$$

where μ_e is an effective viscosity, μ is the fluid velocity, K is the permeability, and G is the applied pressure gradient.

We define dimensionless variables

$$M = \frac{\mu_e}{\mu}, \quad D_a = \frac{K}{a^2}, \quad x = \frac{\bar{x}}{P_e a}, \quad y = \frac{\bar{y}}{a}, \quad u = \frac{\mu\bar{u}}{Ga^2}, \quad P_e = \frac{\rho c_p a^3 G}{\mu k}, \tag{2}$$

where M is the viscosity ratio, D_a the Darcy number, P_e the Peclet number, k the thermal conductivity and ρ the fluid density.

The dimensionless form of Eq. (1) is

$$M\frac{d^2u}{dy^2} - \frac{u}{D_a} + 1 = 0 \quad u(0) = 0, \quad u(1) = 0. \tag{3}$$

Using algebraic package (MAPLE), the solution of the equation (3) is given as

$$U(y) = \frac{1}{s^2}\Big[(1-\cosh(ys)) + (\cosh(s)-1)\frac{\sinh(ys)}{\sinh(s)}\Big], \tag{4}$$

where

$$s = \Big(1/MD_a\Big)^{1/2}. \tag{5}$$

It will be noted that, M and D_a appear only in the combination of M times D_a, hence, without loss of generality, we take $M = 1$ in our analysis.

Using algebraic package (taylor()) in MAPLE the Taylor expansion of Eq.(4) (for large D_a) yeilds

$$u(y) = \frac{(y-y^2)}{2} + \Big(-\frac{1}{24}y^4 + \frac{y^3}{12} - \frac{y}{24}\Big)s^2 + O(s^4), \quad as \quad s \to 0. \tag{6}$$

The steady-state thermal energy equation for the problem is given as

$$\rho c_p \bar{u}\frac{\partial^2 T}{\partial \bar{x}} = k\frac{\partial^2 T}{\partial \bar{y}}. \tag{7}$$

with the following inlet and boundary conditions:

Inlet condition

$$T(0,y) = T_0, \tag{8}$$

Constant heat flux at the lower wall

$$\frac{\partial T}{\partial y}(x,0) = -\frac{q}{k}, \tag{9}$$

Adiabatic wall

$$\frac{\partial T}{\partial y}(x,a) = 0, \tag{10}$$

where T is the absolute temperature and T_0 is the temperature at the inlet. The dimensionless energy equation is given as

$$u\frac{\partial \theta}{\partial x} = \frac{\partial^2 \theta}{\partial y^2}, \tag{11}$$

with

$$\theta(0,1) = 0, \quad \frac{\partial \theta}{\partial y}(x,0) = -1, \quad \frac{\partial \theta}{\partial y}(x,1) = 0, \tag{12}$$

where the dimensionless temperature $\theta = k(T - T_0)/qa$.

The problem is now to solve Eq. (11) subject to the conditions Eq.(12) . We employed the analytical method of separation of variables. Let

$$u\frac{\partial \theta}{\partial x} = \frac{\partial^2 \theta}{\partial y^2} = \lambda, \tag{13}$$

then

$$\theta(x, y) = x\lambda + A(y), \tag{14}$$

where

$$\frac{d^2 A}{dy^2} = \lambda \hat{u}. \tag{15}$$

The above equation is solved completely and the integration constants were obtained from conditions (12). We obtain

$$\theta(x, y) = \frac{-120x}{s^2 - 10} + \frac{30y^4 - 60y^3 + s^2y^6 - 3s^2y^5 + 5s^2y^3 + 60y - 6ys^2 - 30 + 3s^2}{6(s^2 - 10)}. \tag{16}$$

Entropy Generation Rate

According to Mahmud and Fraser[10], the entropy generation rate is define as

$$E_G = \frac{k}{T_0^2}\left[\Big(\frac{\partial T}{\partial \bar{x}}\Big)^2 + \Big(\frac{\partial T}{\partial \bar{y}^2}\Big)^2\right] + \frac{\mu}{T_0}\Big(\frac{\partial u}{\partial \bar{y}}\Big)^2. \tag{17}$$

The dimensionless entropy generation number may be defined by the following relationship:

$$N_s = \frac{kT_0^2}{q^2}E_G. \tag{18}$$

In terms of the dimensionless velocity and temperature, the entropy generation number becomes

$$N_s = \frac{1}{P_e^2}\left(\frac{\partial \theta}{\partial x}\right)^2 + \left(\frac{\partial \theta}{\partial y}\right)^2 + \frac{B_r}{\Omega}\left(\frac{\partial u}{\partial y}\right)^2 = N_x + N_y + N_f, \tag{19}$$

where the dimensionless parameters $B_r = G^2a^3/q\mu$ is the Brinkman number, $\Omega = qa/kT_0$ the dimensionless temperature difference. N_x and N_y are the entropy generation by heat transfer due to both axial and transverse heat conduction respectively and N_f is the entropy generation due to fluid friction.

In convective problem, both fluid friction and heat transfer contribute to the rate of entropy generation. In order to have an idea whether fluid friction or heat transfer entropy generation dominates, a criterion known as the irreversibility ratio defined by ϕ is utilised, where

$$\phi = \frac{N_f}{N_x + N_y}. \tag{20}$$

For $0 \leq \phi < 1$ implies that heat transfer irreversibility dominates and fluid friction dominates when $\phi > 1$. The case where both the heat transfer and fluid friction have the same contribution for entropy generation is characterised by $\phi = 1$

Results and Discussions

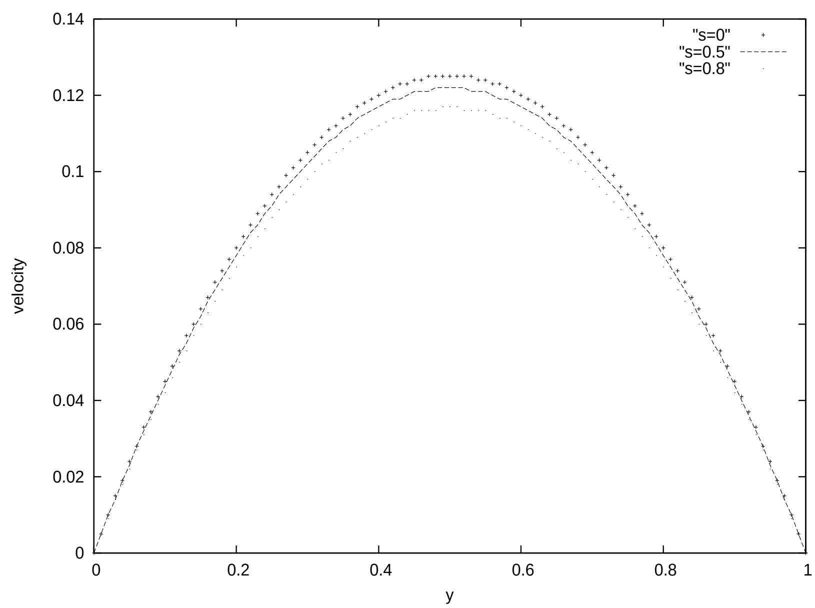

Figure 2: Velocity profiles for different values of s

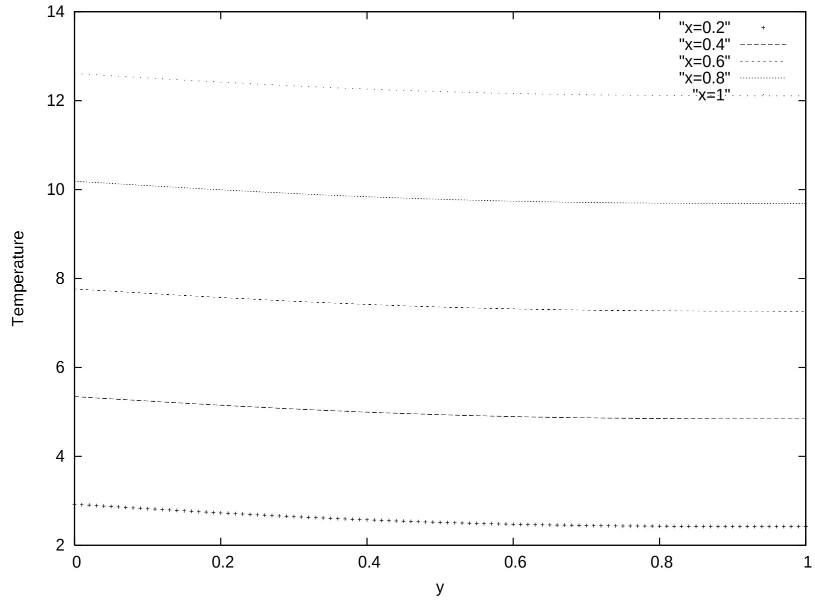

Figure 3: Temperature profiles for different values of x with $s = 0.3$

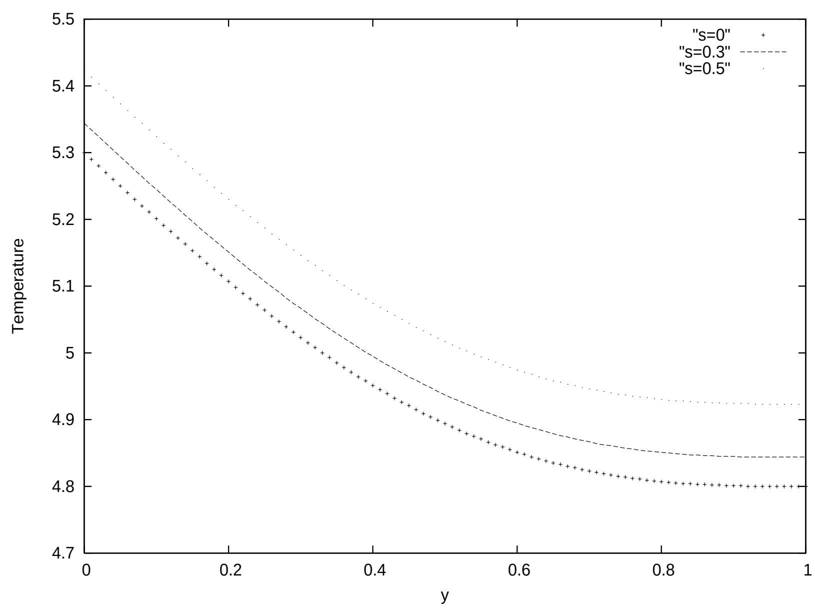

Figure 4: Temperature profiles for different values of s with $x = 0.4$

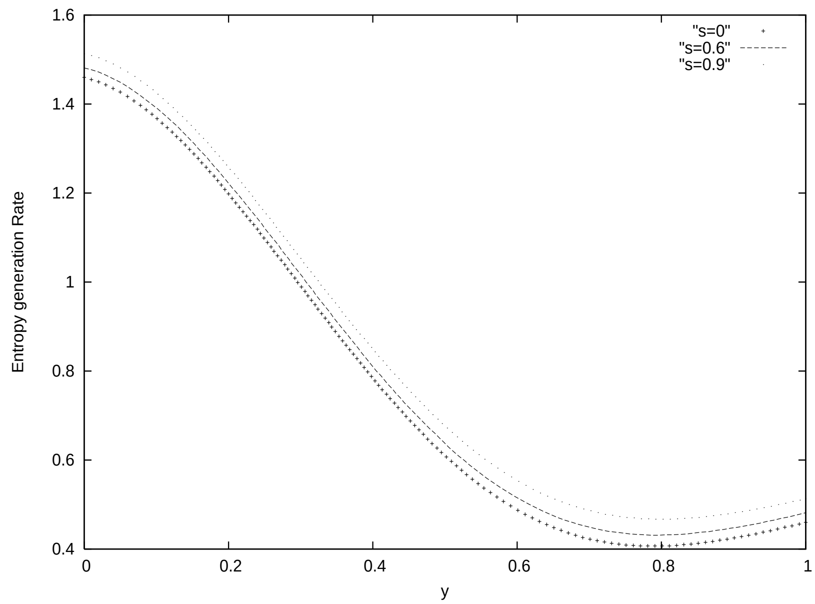

Figure 5: Entropy generation number for different values of s ($P_e = 20$ and $B_r\Omega^{-1} = 0.4$)

Fig.2 shows a parabolic velocity profile across the channel with maximum velocity along the centerline of the channel. The case of $s = 0$ $(s = 1/\sqrt{D})$ coincides with the well known plane Poiseuille flow. It is observed that fluid velocity decreases as porous media permeability decreases (s increases). Fig.3 shows the temperature profiles across the channel for different axial distance. We observed that the fluid temperature increases downstream i.e. axially and decreases transversely across the channel. In Fig. (4) we observed that the fluid temperature decreases in the transverse direction and increases with a decrease in porous media permeability.

The spartial distribution of the entropy generation number for different values of s is plotted in Fig 5. It is interesting to note that entropy generation rate decreases in transverse direction and increases with a decrease in porous media permeability. Such result is expected because high restrictive medium would lead to more disorderliness in the fluid particle. Fig 6 shows the spartial distribution of the entropy generation number for different group parameters. For all values of the group parameters, the entropy generation rate decreases in the transverse direction from the lower wall towards the channel centerline and gradually increases towards the upper wall. This clearly implies that viscous dissipation has no effect on the entropy generation rate at the centerline of a channel filled with porous media.

Graph of Irreversibility ration for different values of B_r For a specific case of $s = 0.5$, and $P_e = 20$, irreversibility ratio is plotted in Fig7. as a function of transverse distance (y) for different group param-

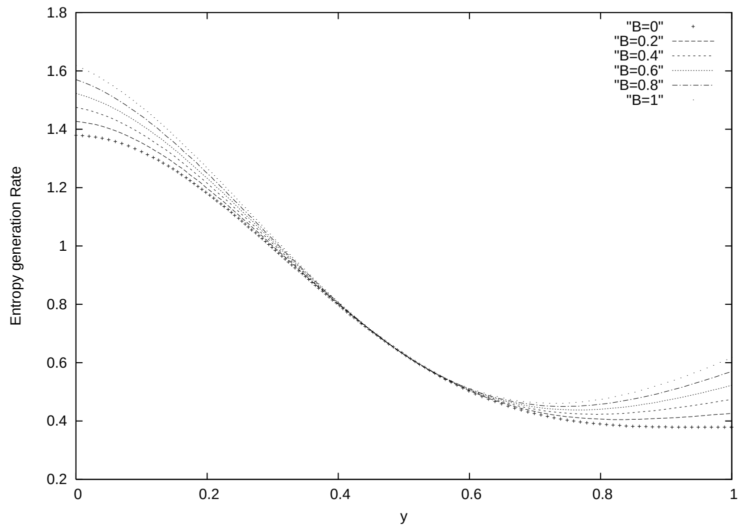

Figure 6: Entropy generation number for different values of $B = B_r\Omega^{-1}$ ($P_e = 20$ and $s = 0.5$)

eters (B_r/Ω). The group parameter is an important dimensionless number for irriversibility analysis. It determines the relative importance of viscous effects to temperature gradient entropy generation. Irreversibility ratio profile is asymmetric about the centerline of the channel due to the asymmetric temperature distribution. For all group parameters, each wall acts as a strong concetrator of irriversibility because of the high near-wall gradients of velocity and temperature. Maximum irreversibility ration occurs near the adiabatic wall fo all group parameters. Fluid friction irreversibility is zero at channel centerline($y = 0.5$) due to zero velocity gradient ($\partial u/\partial y$). Also irreversibility ratio (ϕ) is independent of the group parameter at y=0.5. Therefore, the magnitude of irreversibility ratio is same at centerline of the channel for all group parameters. Minimum irreversibility ratio occur very near where the temperature gradient is zero. Generally, it is observed that an increase in group parameter strengthens the effect of fluid friction irreversibility, but heat transfer irreversibility dominates over fluid friction irreversibility (i.e. $0 \leq \phi < 1$).

Conclusion

This paper presents the application of the second law of thermodynamics to the flow in a channel filled with saturated porous media. The velocity and temperture profiles are obtained and use to compute the entropy generation number and the irreversibility ratio for large Darcy number (D_a) and group parameter ($B_r\Omega^{-1}$). Generally, our result shows that heat transfer irreversibility dominates over fluid friction irreversibility and viscous dissipation has no effect on the entropy generation rate at the centerline of the

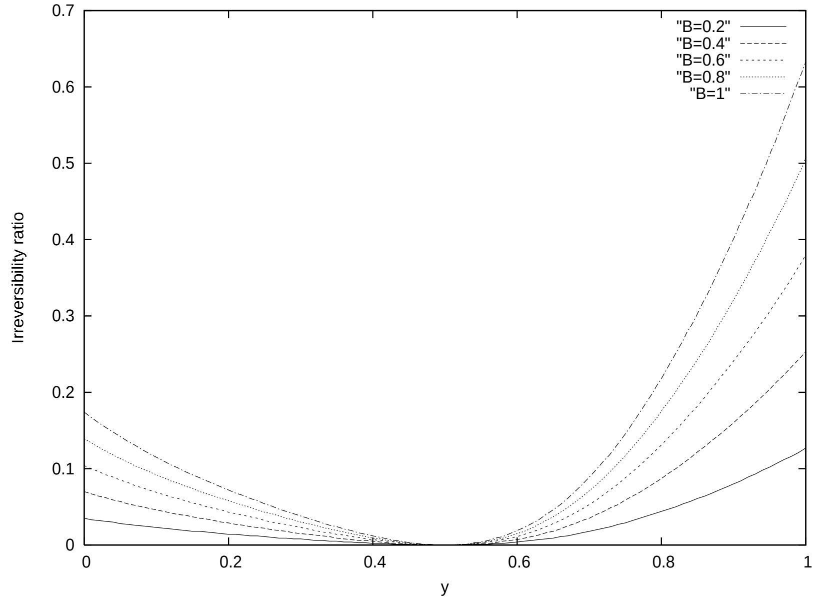

Figure 7: Irreversibility ratio for different values of $B_r\Omega^{-1}$ ($s = 0.5$ and $P_e = 20.$)

channel.

Acknowledgement

The support received from African Institute for Mathematical Sciences (AIMS) in Cape Town and the Department of Applied Mathematics, University of Limpopo, South Africa are highly appreciated.

References

1. Arpaci, V. S.. Radiative entropy production - lost heat into entropy.*Int. J. Heat Mass Transfer* **1993**, 36, 4193-4197.

2. Bejan, A. Second law analysis in heat transfer.*Energy - The Int. J.***1980** 5, 721 732.

3. Bejan, A. Entropy Generation Through Heat and Fluid Flow.*John Wiley & Sons. Inc.: Canada* **1994**, Chapter 5, p 98.

4. Bejan, A.. Entropy Generation Minimization, CRC Press Flow. *John Wiley & Sons. Inc.: Canada* **1996**, Chapter 5, p 98.

5. Bejan, A. Entropy Generation Minimization, *CRC Press: USA* **1996.**

6. Erbay, L.B.; Altaç, Z.; Sülü, B. Entropy Generation in a Square Enclosure Heated From a Vertical Lateral Wall.*Proceedings of the 15th International Symposium on Efficiency, Costs, Optimization, Simulation and Environmental Aspects of Energy Systems* **2002**, 3, 1609-1616.

7. Krane, R. J. A. Second law analysis of the optimum design and operation of thermal energy storage systems. *Int. J. Heat Mass Transfer* **1987**, 30, 43-57.

8. Latife, B. E; Mehmet, S. E.; Birsen, S.; Yalcum, M. M. Entropy generation during fluid flow between two parallel plates with moving bottom plate. *Entropy* **2003**, 5, 506-518.

9. Mahmud, S. and Fraser, R. A. Thermodynamic analysis of flow and heat transfer inside channel with two parallel plates. *Exergy, an International Journal* **2002**, 2, 140-146.

10. Mahmud, S. and Fraser, R. A. The second law analysis in fundamental convective heat transfer problems. *Int. J. of Thermal Sciences* **2002**, 42 (2), 177-186.

11. Nag, P.K. and Kumar, N. Second law optimization of convective heat transfer through a duct with constant heat flux. *Int. J. Energy Research* **1989** , 13 (5), 537-543.

12. Makinde, O. D. Exothermic explosions in a slab: A case study of series summation technique. *Int. Comm. Heat and Mass Transfer* **2004**,31,8,1227-1231.

13. Narusawa, U. The second law analysis of mixed convection in rectangular ducts. *Heat and Mass Transfer* **2001** , 37, 197-203.

14. Nield, D. A.;Kuznetsov, A. V.; Ming, X. Thermally developing forced convection in a porous medium: parallel plate channel with walls at uniform temperature, with axial conduction and viscous dissipation effects. *Int. J. Heat and Mass Transfer* **2003**, 46, 643-651.

15. Rott, N. Themoacoustics .*Adv. Appl. Mech.* **1980**, 20, 135-175.

16. Sahin, A.Z. Irreversibilities in various duct geometries with constant wall heat flux and laminar flow. *Energy, The International J.* **1998**, 23 (6), 465-473.

17. Sahin, A.Z. Entropy generation in turbulent liquid flow through a smooth duct subjected to constant wall temperature.*Int. J. Heat and Mass Transfer* **2000** , 43, 1469-1478.

18. Sahin, A.Z. Entropy generation and pumping power in a turbulent fluid flow through a smooth pipe subjected to constant heat flux. *Exergy, an International Journal* **2002** , 2, 314-321.

19. Salah, S. and Soraya, A. Second law analysis of laminar falling liquid film along an inclined heated plate. *Int. Comm. Heat Mass Transfer* **2004**, 31, No. 6, 879-886.

20. Swift, G. W. Themoacoustics: A unifying perspective for some engines and refrigerators , *ASA Publication, New York*,**2002**.

21. Syeda, H. T., Shohel, M. Entropy generation in a verical concentric channel with temperature dependent viscosity. *Int. Comm. Heat Mass Transfer* **2002** 29, No. 7, 907-918.
